HHS Public Access

Author manuscript

Mol Microbiol. Author manuscript; available in PMC 2016 October 01.

Published in final edited form as:

Mol Microbiol. 2015 October ; 98(1): 175–192. doi:10.1111/mmi.13114.

CdiA promotes receptor-independent intercellular adhesion

Zachary C. Ruhe[1], **Loni Townsley**[2], **Adam B. Wallace**[1], **Andrew King**[3], **Marjan W. Van der Woude**[3], **David A. Low**[1,4], **Fitnat H. Yildiz**[2], and **Christopher S. Hayes**[1,4,†]

[1]Department of Molecular, Cellular and Developmental Biology, University of California, Santa Barbara, Santa Barbara, CA 93106-9625, USA

[2]Department of Microbiology and Environmental Toxicology, University of California, Santa Cruz, Santa Cruz, CA 95064, USA

[3]Centre for Immunology and Infection, Hull York Medical School and the Department of Biology, University of York, YO10 5DD, York, UK

[4]Biomolecular Science and Engineering Program, University of California, University of California, Santa Barbara, Santa Barbara, CA 93106-9625, USA

Summary

CdiB/CdiA proteins mediate inter-bacterial competition in a process termed contact-dependent growth inhibition (CDI). Filamentous CdiA exoproteins extend from CDI$^+$ cells and bind specific receptors to deliver toxins into susceptible target bacteria. CDI has also been implicated in auto-aggregation and biofilm formation in several species, but the contribution of CdiA-receptor interactions to these multi-cellular behaviors has not been examined. Using *Escherichia coli* isolate EC93 as a model, we show that *cdiA* and *bamA* receptor mutants are defective in biofilm formation, suggesting a prominent role for CdiA-BamA mediated cell-cell adhesion. However, CdiA also promotes auto-aggregation in a BamA-independent manner, indicating that the exoprotein possesses an additional adhesin activity. Cells must express CdiA in order to participate in BamA-independent aggregates, suggesting that adhesion could be mediated by homotypic CdiA-CdiA interactions. The BamA-dependent and BamA-independent interaction domains map to distinct regions within the CdiA filament. Thus, CdiA orchestrates a collective behavior that is independent of its growth-inhibition activity. This adhesion should enable "greenbeard" discrimination, in which genetically unrelated individuals cooperate with one another based on a single shared trait. This kind-selective social behavior could provide immediate fitness benefits to bacteria that acquire the systems through horizontal gene transfer.

Keywords

contact-dependent growth inhibition; kind-selection; self/non-self recognition; toxin/immunity proteins; type V secretion systems

[†]Corresponding author, Ph: (805) 893-2028, chayes@lifesci.ucsb.edu.

Introduction

Although they are often regarded as isolated and autonomous unicellular organisms, bacteria possess a number of molecular systems that mediate both cooperative and antagonistic relationships with other microorganisms. Contact-dependent growth inhibition (CDI) is one important mechanism of inter-cellular competition that is commonly found in pathogenic Gram-negative bacteria (Aoki *et al.*, 2010, Hayes *et al.*, 2014, Ruhe *et al.*, 2013a). CDI is a function of CdiB/CdiA two-partner secretion (TPS) proteins, which inhibit the growth of neighboring bacteria upon direct cell-to-cell contact (Hayes et al., 2014, Ruhe et al., 2013a). CdiB is an Omp85 outer-membrane β-barrel protein that exports and assembles CdiA effectors onto the cell surface (Baud *et al.*, 2014, Jacob-Dubuisson *et al.*, 2013). CdiA proteins are very large, ranging from 180 – 630 kDa, and are predicted to form parallel β-helical filaments that extend several hundred angstroms to bind specific receptors on susceptible target bacteria (Kajava *et al.*, 2001, Hayes *et al.*, 2010, Hayes et al., 2014). Upon binding its receptor, CdiA delivers its C-terminal toxin domain (CdiA-CT) into the target cell to inhibit growth. Because CDI^+ strains express receptors for their own CdiA effectors, they also receive toxin domains from adjacent sibling cells (Aoki *et al.*, 2005, Aoki *et al.*, 2008, Aoki et al., 2010, Nikolakakis *et al.*, 2012, Anderson *et al.*, 2012, Arenas *et al.*, 2013, Beck *et al.*, 2014). Though CDI^+ cells exchange toxins with one another, they are protected from growth inhibition by small CdiI immunity proteins encoded immediately downstream of *cdiA*. CdiI binds directly to the CdiA-CT domain and neutralizes toxin activity (Aoki et al., 2010, Beck et al., 2014, Morse *et al.*, 2012, Nikolakakis et al., 2012). Thus, CdiA is deployed to suppress the growth of competing bacteria, but isogenic sibling cells are immune to the delivered toxins.

During the initial characterization of CDI in *Escherichia coli* isolate EC93, Aoki *et al*. found that expression of the $cdiBAI^{EC93}$ gene cluster causes laboratory strains of *E. coli* to auto-aggregate (Aoki et al., 2005). Cell-cell adhesion activity has also been reported for CdiA proteins from several other bacterial species. Before CDI was recognized as a competition system, Collmer and colleagues found that HecA promotes aggregation in *Erwinia chrysanthemii* EC16 cells and that this function is required for full virulence on a plant host (Rojas *et al.*, 2002). HecA is a CdiA homolog and its C-terminal domain has a colicin E3-like nuclease activity that is specifically blocked by the VirA immunity protein (Walker*et al.*, 2004, Beck et al., 2014). These observations indicate that *E. chrysanthemii* EC16 probably uses HecA in inter-cellular competition, but the system also coordinates multi-cellular behavior during host invasion. This may be a general feature of CDI in plant pathogens, because CdiA proteins from *Xylella fastidiosa* (HxfB) and *Xanthomonas axonopodis* (XacFhaB) have also been implicated in virulence and biofilm formation (Guilhabert & Kirkpatrick, 2005, Gottig *et al.*, 2009). HrpA from *Neisseria meningitidis* is yet another CdiA protein that is required for biofilm formation (Neil & Apicella, 2009), and *hrpA* mutants show decreased intracellular survival and escape from infected mammalian cells (Tala *et al.*, 2008). Together, these studies demonstrate that CDI has a broader role in bacterial biology, promoting cooperative interactions between isogenic CDI^+ cells during colonization of eukaryotic hosts.

Because CDI entails specific binding interactions between bacterial cells, the adhesin activity of CdiA represents the most direct mechanism to control biofilm architecture. However, previous studiesraise the possibility that CDI influences biofilm formation in other indirect ways. Gottig *et al.* found that *X. axonopodis* mutants lacking XacFhaB are hyper-motile due to the over-production of xanthan exopolysaccharides that are required for swarming motility (Gottig et al., 2009). In this instance, excessive extracellular polysaccharide has the paradoxical effect of suppressing biofilm formation by facilitating rapid migration of cells from one another. Intriguingly, Cotter and colleagues have recently reported that CdiA-CT^{E264} toxin activity is required for biofilm formation in *Burkholderia thailandensis* E264 (Anderson et al., 2012, Garcia *et al.*, 2013). Wild-type *B. thailandensis* cells are immune to the DNase activity of CdiA-CT^{E264} (Anderson et al., 2012, Nikolakakis et al., 2012), so this domain's role in biofilm formation must be distinct from its growth-inhibition function. Because extracellular DNA is an important component of the *B. thailandensis* biofilm matrix, it has been suggested that the CdiA-CT^{E264} toxin could modulate the physical properties of matrix DNA (Garcia et al., 2013). Similarly, the tRNase activity of CdiA-CT^{UPEC536} appears to influence biofilm formation in uropathogenic *E. coli* (Diner *et al.*, 2012). Taken together, these observations have led to the hypothesis that CdiA-CT domains possess additional signaling functions when delivered into immune sibling cells (Diner et al., 2012). In this model, CDI functions as a quorum-sensing mechanism to monitor the proximity/density of sibling cells and use that information to modulate gene expression through unknown signal transduction pathways.

Here, we use *E. coli* EC93 as a model to study the role of CDI in biofilm formation. The CDI^{EC93} system is well characterized and CdiA^{EC93}-receptor interactions are understood at the molecular level. CdiA^{EC93} exploits the outer-membrane protein BamA as its receptor (Aoki et al., 2008). BamA is an essential Omp85 protein required for the assembly of all β-barrel proteins in Gram-negative bacteria (Voulhoux *et al.*, 2003, Wu *et al.*, 2005, Doerrler & Raetz, 2005, Werner & Misra, 2005). Although BamA is conserved between enterobacteria, the extracellular loop regions recognized by CdiA^{EC93} are variable between species (Smith *et al.*, 2007, Ruhe *et al.*, 2013b). Therefore, CdiA^{EC93} does not bind to BamA proteins from other bacteria, and *E. coli* cells that express heterologous *bamA* are resistant to inhibition by the CDI^{EC93} system (Ruhe et al., 2013b). In accord with previous studies, we find that *E. coli* EC93 Δ*cdiA* mutants are defective in biofilm formation. However, these defects are not due to changes in biofilm-associated gene expression, nor are they dependent on the CdiA-CT toxin region of CdiA^{EC93}. Instead, CdiA^{EC93} promotes biofilm formation directly by mediating inter-cellular adhesion between neighboring cells. Remarkably, CDI^{+} cells that express heterologous *bamA* genes still auto-aggregate, indicating that the CdiA^{EC93}-BamA^{Eco} binding interaction is not strictly required for CDI-dependent inter-cellular adhesion. We provide evidence that CdiA^{EC93} possesses an additional adhesion domain that is distinct from the BamA^{Eco}-binding region. Together, these data demonstrate that CdiA expressing bacteria can physically interact with one another in a receptor-independent manner. The proposed CdiA-CdiA binding interactions should facilitate cooperative behaviors between CDI^{+} bacteria and could promote the dispersal of *cdi* loci through horizontal gene transfer.

Results

EC93 Δ*cdiA* mutants are defective for biofilm formation

To determine whether CDI plays a role in *E. coli* EC93 biofilm formation, we cultured *cdiA*$^+$ and Δ*cdiA* strains in 96-well polystyrene plates over a 10 h time period and quantified biofilm mass. Wild-type *cdiA*$^+$ cells adhered to the plates within four h, then displayed a reproducible decrease in biofilm mass at 8 h, after which biomass again increased (Fig. 1A). The Δ*cdiA* mutant initially adhered to the plate with similar kinetics as *cdiA*$^+$ cells, but generated significantly less biofilm mass over the entire time course (Fig. 1A). To examine biofilm architecture, we used confocal laser-scanning microscopy (CLSM) to visualize EC93 communities grown in static chambers. We observed a similar biofilm defect for Δ*cdiA* cells under these conditions, and quantification of biomass ($P = 0.022$) and average biofilm thickness ($P < 0.0001$) revealed significant differences between *cdiA*$^+$ and Δ*cdiA* strains (Fig. 1B & Table 1). The C-terminal toxin domain of CdiA plays an important role in *B. thailandensis* biofilms (Garcia et al., 2013), so we tested whether deletion of the CdiA-CT^{EC93} region has a similar effect in *E. coli* EC93. We truncated CdiA^{EC93} after residue Ala2909, which demarcates the N-terminal boundary of the toxin domain (Aoki et al., 2010). The resulting *cdiA(A2909)* strain produced nearly as much biofilm mass as wild-type cells in polystyrene wells (Fig. 1A), though there were subtle decreases in biofilm mass ($P = 0.09$) and average thickness ($P = 0.53$) revealed by CLSM analysis of communities grown is static chambers (Fig. 1B & Table 1). These data are consistent with reports that *cdi* genes are important for biofilm formation in several other Gram-negative bacteria. However, *E. coli* EC93 differs from *B. thailandensis* E264 in that the CdiA-CT^{EC93} domain is not required to form a biofilm community.

EC93 Δ*cdiA* mutants have no defects in growth rate, motility or biofilm gene expression

A number of factors could contribute to reduced biofilm formation in Δ*cdiA* mutants. We first tested whether the phenotype results from a decreased growth rate and found that *cdiA*$^+$ and Δ*cdiA* cells grow at identical rates (Fig. S1A). Cell motility and the production of extracellular polysaccharide matrices also play key roles in biofilm formation; and previous work shows that *X. axonopodis cdiA* mutants are hyper-motile and have perturbed extracellular polysaccharide metabolism (Gottig et al., 2009). We examined the motility of Δ*cdiA* mutants on swim plates and found no significant changes from that of *cdiA*$^+$ cells ($P = 0.3378$, Figs. S1B & S1C). Moreover, quantitative real-time PCR (qRT-PCR) analysis revealed that the levels of *fliC* transcripts (which encode flagellin monomers) were nearly identical in sessile populations of *cdiA*$^+$ and Δ*cdiA* cells (Fig. S1D and data not shown). Thus, *cdiA*$^+$ and Δ*cdiA* cells display similar flagellum synthesis and motility. We then examined the expression of genes required for the production poly-N-acetyl-D-glucosamine (PGA), cellulose and colanic acid, which are common polysaccharides used in the extracellular matrix of *E. coli* biofilms (Itoh *et al.*, 2005, Wang *et al.*, 2004, Serra *et al.*, 2013, Danese *et al.*, 2000, Prigent-Combaret *et al.*, 1999). Because *fliC* message levels were equivalent in the *cdiA*$^+$ and Δ*cdiA* backgrounds, we used this transcript as a reference standard for $\Delta\Delta C_T$ analyses as described (Schmittgen & Livak, 2008). We isolated total RNA from biofilms grown on polystyrene wells for four h and quantified the relative levels of *pgaA*, *bcsA* and *wcaA* transcripts to monitor PGA, cellulose and colanic acid biosynthetic

pathways, respectively. The *pga* message was essentially unaltered in Δ*cdiA* mutants, whereas *bcsA* and *wcaA* transcripts were elevated in Δ*cdiA* cells compared to wild-type (Fig. S1D). Together, these findings indicate that the Δ*cdiA* biofilm defect cannot be attributed to differences in growth rate, cell motility or decreased expression of extracellular matrix genes.

CdiA-BamA binding contributes to E. coli EC93 biofilm formation—CdiA (Aoki et al., 2005) and other two-partner exoproteins (Locht *et al.*, 1993) have well-characterized adhesin properties, suggesting that $CdiA^{EC93}$ might influence biofilm formation through its binding interactions with BamA. To test this model, we incubated wild-type $cdiA^{+}$ cells in polystyrene wells for 2 h to allow initial surface attachment, then supplemented the culture with proteinase K (20 μg mL^{-1}) and continued the incubation for 8 h. Our previous studies have shown that this treatment is sufficient to remove $CdiA^{EC93}$ from the cell surface (Ruhe *et al.*, 2014). Moreover, this concentration of proteinase K had no effect on *E. coli* EC93 $cdiA^{+}$ or Δ*cdiA* cell growth (Fig. S2). As anticipated, the biofilm produced by proteinase-treated cells was similar to that of Δ*cdiA* mutants and had significantly less biomass than untreated $cdiA^{+}$ cells (Fig. 1A). This result suggests that extracellular protein is important for *E. coli* EC93 biofilm formation, and supports a model in which $CdiA^{EC93}$ functions as an adhesin and/or a proteinaceous matrix to hold cells together.

Because *E. coli* EC93 cells express $BamA^{Eco}$ receptors, we reasoned that $CdiA^{EC93}$-$BamA^{Eco}$ binding interactions should contribute significantly to biofilm assembly. To test this model, we examined *E. coli* EC93 cells in which $bamA^{Eco}$ is replaced with the $bamA^{LT2}$ gene from *Salmonella* Typhimurium LT2. $BamA^{LT2}$ is not recognized as a receptor by $CdiA^{EC93}$ (Ruhe et al., 2014, Ruhe et al., 2013b), and therefore $bamA^{LT2}$ cells cannot form cell-cell aggregates through CdiA-receptor binding interactions. To demonstrate that EC93 $bamA^{LT2}$ cells lack a functional $CdiA^{EC93}$ receptor, we deleted the $cdiI^{EC93}$ immunity gene to generate EC93 $bamA^{LT2}$ Δ*cdiI* cells. The resulting strain retained full CDI activity in competition co-cultures with *E. coli* X90 target bacteria (Fig. 2A), indicating that it continues to deploy $CdiA^{EC93}$ effectors. Moreover, plasmid-borne $bamA^{Eco}$ could not be introduced into EC93 $bamA^{LT2}$ Δ*cdiI* cells unless they were first provided with a copy of the $cdiI^{EC93}$ immunity gene on a compatible plasmid (Fig. 2B). Together, these experiments show that EC93 $bamA^{LT2}$ cells produce a functional CDI^{EC93} apparatus, but lack the $CdiA^{EC93}$ receptor and therefore cannot be targeted by sibling cells. Surprisingly, the EC93 $bamA^{LT2}$ strain did not phenocopy the Δ*cdiA* mutant in a static biofilm assay. Instead, $bamA^{LT2}$ cells produced more biofilm mass in polystyrene wells than the Δ*cdiA* mutant and nearly as much as wild-type EC93 cells (Fig. 1A). However, EC93 $bamA^{LT2}$ biofilms grown in static chambers contained less average biomass ($P = 0.035$) and had reduced biofilm thickness ($P = 0.15$) compared to wild-type EC93 (Fig. 1B & Table 1). These data indicate that $CdiA^{EC93}$-$BamA^{Eco}$ binding contributes to biofilm formation, but CDI also appears to facilitate cell-cell interactions in a receptor-independent manner.

Receptor-independent auto-aggregation of CDI^{+} cells—Expression of the $cdiBAI^{EC93}$ gene cluster causes auto-aggregation of laboratory *E. coli* K-12 strains (Aoki et al., 2005). Because auto-aggregation and biofilm formation are often related phenomena, we

examined whether BamA^{Eco} is strictly required for CDI-dependent aggregation. We first confirmed that *cdiBAI*^{EC93} expression is sufficient to promote auto-aggregation in *E. coli* EPI100 cells. The *cdiBAI*^{EC93} gene cluster was placed under the control of an IPTG-inducible promoter and auto-aggregation was monitored by measuring the optical density (at 600 nm) at the surface of standing liquid cultures as a function of time. Because aggregates sediment more rapidly than individual cells, OD_{600} values decline at a faster rate when cells aggregate. In the absence of IPTG, cell density at the culture surface remained nearly constant over 4 h (Fig. 3A). However, upon induction with IPTG, the culture showed significant sedimentation over the same time period (Figs. 3A & 3B). We then introduced the IPTG-inducible *cdiBAI*^{EC93} expression construct into *E. coli* EPI100 Δ*bamA* cells that express plasmid-borne *bamA*^{ECL} from *Enterobacter cloacae* ATCC 13047. Like BamA^{LT2}, the BamA^{ECL} protein is not a receptor for CdiA^{EC93} (Ruhe et al., 2014, Ruhe et al., 2013b). We again monitored cell aggregation through sedimentation and surprisingly found that CDI$^+$ *bamA*^{ECL} cells fell out of suspension almost as rapidly as CDI$^+$ *bamA*^{Eco} cells (Figs. 3A & 3B). Thus, expression of the *cdiBAI*^{EC93} gene cluster promotes auto-aggregation in a BamA^{Eco}-independent maxnner.

Cells must express CdiA^{EC93} to participate in cellular aggregates—CdiA^{EC93} fragments are released into the growth medium (Aoki et al., 2005), raising the possibility that these peptides form a β-amyloid-like matrix that non-specifically binds bacteria together. If so, then CDI$^+$ bacteria should be able to capture CDI$^-$ cells in the aggregates. We tested this prediction using flow cytometry to detect and quantify cell-cell binding interactions (Aoki et al., 2008, Ruhe et al., 2013b). We generated GFP- and DsRed-labeled EPI100 *bamA*^{ECL} cells, then provided the strains with the *cdiBAI*^{EC93} expression plasmid (CDI$^+$) or an empty vector control (CDI$^-$). As expected, the resulting GFP CDI$^-$, GFP CDI$^+$, DsRed CDI$^-$ and DsRed CDI$^+$ strains showed very low levels of dual green/red fluorescence when analyzed individually by flow cytometry (Fig. 4A). We then mixed GFP- and DsRed-labeled cells at a 1:1 ratio and incubated with shaking to facilitate cell-cell binding. Analysis of the GFP CDI$^-$/DsRed CDI$^-$ co-culture showed that ~1% of the flow events had both green and red fluorescence (Fig. 4B). Similarly, only about 5% of the events had dual fluorescence when CDI$^+$ cells were mixed with a CDI$^-$ population (Fig. 4B). In contrast, approximately 50% of the events exhibited dual fluorescence when GFP-labeled CDI$^+$ cells were mixed with DsRed-labeled CDI$^+$ cells (Fig. 4B). This latter result indicates that bacteria must express CdiA^{EC93} in order to join the aggregates. Moreover, because these strains lack BamA^{Eco} receptors, the cell-cell binding interactions are presumably distinct from those that form between inhibitor and target cells during CDI. This conclusion is supported by forward light scatter analysis, which indicated that CDI$^+$ *bamA*^{Eco} cell aggregates are larger and more heterogenous than the CDI$^+$ *bamA*^{ECL} aggregates (Fig. 5A). Light microscopy also showed that CDI$^+$ *bamA*^{Eco} cells form significantly larger aggregates than CDI$^+$ *bamA*^{ECL} cells (Fig. 5B). By contrast, forward scatter analysis and light microscopy showed that most CDI$^-$ cells exist as isolated individuals, regardless of their *bamA* background (Figs. 5A & 5B). Thus, CdiA^{EC93}-expressing bacteria physically interact in a BamA^{Eco}-independent manner. Because CdiA^{EC93} expression is required to participate in these aggregates, we hypothesized that this cell-cell adhesion is mediated by homotypic CdiA-CdiA binding interactions.

Receptor-dependent and -independent binding regions map to different positions within CdiA^{EC93}—We next sought to determine whether the two adhesin activities are mediated by distinct regions of the CdiA^{EC93} filament. We generated a series of CdiA^{EC93} truncation constructs (Fig. 6A) and analyzed their BamA-binding properties using flow cytometry. Cells expressing CdiA^{EC93} truncated at residues Val2905 and Arg2123 still aggregated specifically with *bamA*^{Eco} target bacteria, but truncation to residue Arg1930 significantly attenuated cell-binding activity (Fig. 6B). Further truncation to residue Asn1319 completely abrogated the ability to bind *bamA*^{Eco} target cells (Fig. 6B). These data indicate that the BamA^{Eco}-binding region lies somewhere within the N-terminal 1930 residues of CdiA^{EC93}. We then tested internal deletion constructs and found that CdiA^{EC93} proteins lacking residues Ser633 – Gly721 and Ser644 – Gly721 retained BamA^{Eco}-binding activity, but deletion of Ala722 – Gly1624 abrogated this activity (Figs. 6A & 6B). This latter results suggests that the BamA^{Eco}-binding region is located between residues Ala722 and Gly1624, but it is also possible that CdiA(ΔAla722-Gly1624) is not secreted or perhaps not assembled properly on the cell surface. Therefore, we analyzed each truncation and deletion variants by immunoblot using polyclonal antibodies against the N-terminal TPS transport domain of CdiA^{EC93}. In general, each CdiA^{EC93} variant accumulated to approximately the same level as wild-type protein, but the CdiA(Asn1319) and CdiA(ΔGly277-Gly721) proteins were much less abundant (Fig. 7). The latter mutation deletes a portion of the TPS transport domain, which is predicted prevent export across the outer membrane. To monitor CdiA^{EC93} secretion, we treated intact cells with proteinase K to degrade extracellular protein and compared them to untreated cells using immunoblot analysis. With the exception of the ΔGly277-Gly721 mutant, all of the variants were sensitive to extracellular protease (Fig. 7), indicating that most of the CdiA^{EC93} variants were exported to the cell surface. These data suggest that CdiA(ΔAla722 – Gly1624) is processed properly and does not bind target bacteria because the BamA^{Eco}-binding region has been deleted.

We then examined CdiA^{EC93} truncation and deletion variants for receptor-independent auto-aggregation. CdiA^{EC93} proteins truncated at Val2905, Arg2123 and Arg1930 all supported auto-aggregation in the *bamA*^{ECL} genetic background, but cells expressing the Asn1319 truncation protein did not sediment (Fig. 6C). Forward scatter analysis also indicated that all truncations except CdiA(Asn1319) promoted auto-aggregation in the *bamA*^{ECL} background (Fig. S3). Sedimentation analysis of the internal deletion variants revealed that CdiA(ΔSer644-Gly721) and CdiA(ΔAla722-Gly1624) support receptor-independent aggregation, whereas the other deletion constructs do not (Fig. 6C). Together, these experiments identified internal deletion constructs that retain specific adhesion activities. CdiA(ΔAla722-Gly1624) does not bind to BamA^{Eco}, but supports receptor-independent auto-aggregation (Figs. 6B & 6C). Conversely, CdiA(ΔSer633-Gly721) specifically binds to BamA^{Eco}, yet lacks auto-aggregation activity (Figs. 6B & 6C). Collectively, these data demonstrate that the BamA^{Eco} and receptor-independent adhesion domains map to different positions on the CdiA^{EC93} filament.

Having localized the receptor-independent adhesion domain to the N-terminal region of CdiA^{EC93}, we asked whether this portion of the filament plays any role in CDI. We used

EPI100 cells that express CdiA^{EC93} deletion variants as inhibitor strains in competition co-cultures with *E. coli* X90 target bacteria. X90 targets grew about 5-fold in mock competitions with CDI^{-} EPI100 cells, but viable X90 cells were reduced ~40,000-fold in co-cultures with EPI100 cells that express full-length CdiA^{EC93} (Fig. 8). Inhibitors that express truncated CdiA(Val3105) were unable to inhibit target cells (Fig. 8), demonstrating that the C-terminal toxin domain is required for growth inhibition. The CdiA(ΔGly277-Gly721) protein also failed to inhibit target bacteria (Fig. 8), consistent with the observation that this effector is not secreted and therefore cannot bind to target cells. In contrast, CdiA(ΔSer633-Gly721) and CdiA(ΔSer644-Gly721) mutants both retained inhibition activity, reducing target-cell counts approximately 600- and 11,000-fold, respectively (Fig. 8). CdiA(ΔAla722-Gly1624), which lacks BamA^{Eco}-binding activity, was unable to inhibit target cells and phenocopied the export-defective (ΔGly277-Gly721) and toxin-deletion (Val3105) mutants (Fig. 8). Taken together, these data show that the two adhesion activities have distinct functions and locations on the CdiA^{EC93} filament. The BamA^{Eco}-binding domain appears to reside between residues Ala722 and Gly1624 and is essential for toxin delivery into target cells. In contrast, the receptor-independent adhesion domain maps to a region N-terminal to Ser644 and is not required for CDI-mediated growth inhibition.

Discussion

TPS and auto-transporter proteins have long been implicated in bacterial biofilm formation (Rojas et al., 2002, Neil & Apicella, 2009, Gottig et al., 2009, Irie *et al.*, 2004, Serra *et al.*, 2011, Anderson et al., 2012). These type V secretion systems often function as adhesins, implying that the secreted exoproteins mediate attachment to the substratum and/or other bacteria during biofilm formation. In addition to directly mediating adhesion, results suggest that CDI modulates biofilm formation indirectly through changes in gene expression (Gottig et al., 2009). Additionally, Cotter and co-workers report that the enzymatic activity of the CdiA-CT^{E264} toxin is required for biofilm formation in *B. thailandensis* E264 (Garcia et al., 2013). In contrast, we find no significant alterations in cell motility or biofilm gene expression in *E. coli* EC93 Δ*cdiA* mutants; and the CdiA-CT^{EC93} region does not appear to play the same critical role in *E. coli* EC93 biofilms as it does in *B. thailandensis*. Presumably, these discrepancies reflect fundamental differences between CDI systems. For example, *E. coli* EC93 expresses its *cdi* genes constitutively (Aoki et al., 2005), whereas the *B. thailandensis* system is regulated by quorum sensing (Majerczyk *et al.*, 2014). Moreover, homology between CdiA^{EC93} and CdiA^{E264} is largely limited to the N-terminal TPS transport domain and the effectors carry unrelated toxin domains (Fig. S4). The CdiA-CT^{E264} region has Mn^{2+}-dependent DNase activity (Garcia et al., 2013, Nikolakakis et al., 2012), whereas the CdiA-CT^{EC93} toxin domain forms membrane pores (Aoki *et al.*, 2009, Ruhe et al., 2014). Garcia *et al.* have suggested that CdiA-CT^{E264} activity could modify the extracellular DNA matrix and thereby promote *B. thailandensis* biofilm formation (Garcia et al., 2013). In contrast, our data suggest that CdiA^{EC93} acts primarily as an adhesin to tether bacterial cells to one another. However, CdiA^{EC93}-expressing cells still auto-aggregate when they lack functional BamA^{Eco} receptors. The simplest explanation for these data is that CdiA^{EC93} possesses an additional adhesion activity. We hypothesize that CdiA^{EC93} may mediate cell adhesion through homotypic interactions, because bacteria must express

CdiA^{EC93} in order to participate in receptor-independent aggregates. Homotypic interactions have been proposed previously for other type V secretion systems, including the Ag43 autotransporter from *E. coli* (Girard *et al.*, 2010) and *Bordetella* FHA (Menozzi *et al.*, 1994). FHA appears to bind several different ligands including mammalian integrins (Ishibashi *et al.*, 1994, Relman *et al.*, 1990). Notably, other CdiA proteins were originally described as adhesins that bind to eukaryotic host cells. MhaB1 and MhaB2 from *Moraxella catarrhalis* were found to increase bacterial association with human epithelial cells in culture (Balder *et al.*, 2007). HrpA from *N. meningitidis* was reported to facilitate adhesion to epithelial cells, though the *hrpA* phenotype is only manifest in lipopolysaccharide-deficient mutant backgrounds (Schmitt *et al.*, 2007). Taken together, these observations suggest that CdiA proteins often possess multiple adhesion domains.

De novo biofilm formation requires that bacteria first adhere to a surface. After this initial attachment phase, cells secrete extracellular matrix molecules, which help bind the bacteria together and allow large three-dimensional structures to be built. EC93 Δ*cdiA* mutants have different initial attachment phenotypes depending on the abiotic substratum. EC93 *cdiA*$^+$ and Δ*cdiA* cells adhere to polystyrene surfaces at similar rates, but Δ*cdiA* mutants appear to have difficulty establishing biofilms on glass surfaces. However, the more profound defect appears to be in biofilm maturation, in accord with previous findings with *N. meningitidis* and *B. thailandensis cdi* mutants (Neil & Apicella, 2009, Anderson et al., 2012, Garcia et al., 2013). Collectively, these observations suggest that CdiA augments cell-cell interactions and reinforces the extracellular matrix. Intriguingly, the *E. coli* EC93 *cdiBAI* locus is linked to a predicted fimbria operon. Fimbriae are adhesive appendages that often mediate attachment to abiotic substrates and are therefore critical for the early stages of biofilm formation. This genetic linkage could perhaps indicate cooperation between the fimbria and CdiA^{EC93} adhesion systems during biofilm formation. We note a similar linkage in uropathogenic *E. coli* strains, where the *cdi* genes are carried on pathogenicity island II together with type I fimbria and the pyelonephritis associated pili (*pap*) genes (Dobrindt *et al.*, 2002). These associations suggest that CDI plays an integral role in biofilm lifestyles, and that its adhesin activities contribute to bacterial virulence and pathogenicity.

CDI provides a mechanism to discriminate neighboring cells through both kin- and kind-selection. Kin are defined as individuals that are related to one another across their entire genomes and whose genetic relationships are the result of direct vertical descent (Strassmann *et al.*, 2011). By contrast, individuals of the same kind are those that share a specific trait – often specified by a single genetic locus – but are not necessarily related at other loci (Strassmann et al., 2011). Adhesion between isogenic CDI$^+$ cells represents a form of kin selection, which increases the relatedness of the population and provides benefits by resisting forces that would disrupt the community. But *E. coli* EC93 cells also have the potential to adhere to other *E. coli* strains, because virtually all isolates carry and express identical *bamA*^{Eco} receptor genes. Thus, the growth-inhibition function of CDI could prevent intrusions by other *E. coli* strains, or conversely allow the CDI$^+$ strain to attach to and invade an established *E. coli* microcolony. In contrast, receptor-independent CdiA-CdiA interactions represent a possible kind-selective mechanism, whereby unrelated bacteria cooperate if they express similar *cdiA* alleles. Strains of *Citrobacter rodentium*,

Salmonella typhi and *Enterobacter cloacae* all encode CdiA proteins that share significant (>50%) sequence identity with $CdiA^{EC93}$ over the homotypic interaction region. In principle, these strains could participate in CdiA-mediated aggregation and cooperate with *E. coli* EC93 cells by co-inhabiting the same biofilm community. Thus, *cdiA* genes may act as so-called greenbeard alleles, which allow individuals to recognize others with the same trait and direct preferential treatment to them (Dawkins, 1976, West & Gardner, 2010, Strassmann et al., 2011). This kind-selective function could be critical for the maintenance and propagation of *cdi* genes, which are usually found within genomic islands and other mobile genetic elements (Poole *et al.*, 2011). Because greenbeard discrimination promotes cooperation between unrelated individuals, it may provide selective pressure to spread *cdi* loci through horizontal gene transfer.

CDI-mediated growth inhibition is usually limited to closely related bacteria (Aoki et al., 2005, Aoki et al., 2010, Nikolakakis et al., 2012, Arenas et al., 2013, Anderson et al., 2012, Beck et al., 2014, Anderson *et al.*, 2014, Koskiniemi *et al.*, 2015). For *E. coli* EC93, the molecular basis of this discrimination is understood and reflects variations in cell-surface epitopes of the BamA receptor between bacterial species (Ruhe et al., 2013b). Therefore, the specificity of CdiA-receptor interactions limits the target-cell range. This feature of CDI makes biological sense if related bacteria are more likely to compete for the same environmental resources. However, these observations raise important questions about the evolution of *cdi* genes, particularly with respect to horizontal gene transfer. The genes encoding CDI systems are often associated with transposable elements and are sometimes encoded within genomic islands, suggesting that *cdi* genes are transferred horizontally between different bacteria. This hypothesis is also consistent with the observation that *cdi* loci are not necessarily found in all strains of a given species (Aoki et al., 2010, Poole et al., 2011). Therefore, if *cdi* genes are transferred between different bacterial species, it is likely that the recipient bacterium will not carry an appropriate surface receptor for the acquired CDI system. Because all characterized CDI systems recognize self receptors, CdiA-receptor interactions probably evolve after the horizontal gene transfer event. This is presumably a slow process, raising the question of what selective pressures allow retention of *cdi* loci in the interim. One possibility is that the toxin/immunity functions of CDI enforce retention. Although CDI toxins cannot be delivered between cells in the absence of a suitable CdiA receptor, synthesis of the CdiA-CT toxin from internal translation initiation sites could stabilize *cdi* genes through an immunity protein addiction mechanism similar that that proposed for type II prokaryotic toxin/antitoxin modules (Jensen & Gerdes, 1995, Wozniak & Waldor, 2009). The results presented here suggest that receptor-independent adhesion could provide an additional selective advantage to cells that have newly acquired *cdi* genes. TPS systems are autonomous and have the potential to function in a variety of Gram-negative bacteria. Therefore, newly acquired *cdiBA* genes could plausibly produce properly assembled CdiB/CdiA complexes on the cell surface, thereby enabling receptor-independent auto-aggregation. If these auto-adhesive properties provide a significant fitness benefit, then bacteria that retain the *cdi* genes would derive a selective advantage thereby providing the opportunity for *cdiA* to acquire new receptor-binding function.

Materials and Methods

Strains and growth conditions

Bacterial strains used in this study are listed in Table 2. Bacteria were routinely grown in LB broth or LB agar at 37 °C unless otherwise noted. Growth media was supplemented with antibiotics (ampicillin, 100 μg mL^{-1}; kanamycin, 50 μg mL^{-1}; tetracycline 12.5 μg mL^{-1}) where indicated. *E. coli* EC93 Δ*cdiA* (CH10094) and $bamA^{LT2}$ (CH10053) strains have been described previously (Ruhe et al., 2013b, Ruhe et al., 2014). The toxin-encoding region of *cdiA* was deleted from *E. coli* EC93 to generate strain CH10024. Regions of upstream and downstream of the *cdiA-CT* sequence were amplified with primers ΔcdiA(CT)-up-Sac/ΔcdiA(CT)-up-Bam and ΔcdiA-dn-Eco/ΔcdiA-dn-Xho, respectively (Table S1). The resulting products were sequentially ligated to plasmid pKAN (Hayes *et al.*, 2002) to generate pKAN-*cdiA*Δ*CT* (Table 2). The SacI/EcoRI fragment from plasmid pKAN-*cdiA*Δ*CT* was introduced into *E. coli* EC93 cells that express phage λ Red recombinase genes from plasmid pSIM6 as described (Thomason *et al.*, 2007). The FRT-flanked kanamycin-resistance cassette was removed using FLP recombinase as described (Cherepanov & Wackernagel, 1995). The *cdiI* gene was deleted from *E. coli* EC93 $bamA^{LT2}$ cells (strain CH10060) using essentially the same approach. Upstream and downstream homology regions were amplified using primers EC93-cdiI(KO)-Sac/EC93-cdiI(KO)-Bam and EC93-cdiI(KO)-Eco/EC93-cdiI(KO)-Xho, respectively. The two products were sequentially ligated to plasmid pKAN to generate plasmid pKAN-Δ*cdiI*. The SacI/XhoI fragment from plasmid pKAN-Δ*cdiI* was introduced into *E. coli* CH10060 cells that express phage λ Red recombinase genes.

Motility was assayed on freshly prepared tryptone broth agar (0.4% agar). Overnight cultures were adjusted to OD_{600} = 1.0 and 10 μL of the suspension was spotted onto the center of the plate. Plates were incubated in humid chambers at 37 °C for 12 h. Bacterial competition co-cultures were conducted in LB media without antibiotics. Inhibitors and target bacteria (*E. coli* X90) were grown individually to mid-log phase at 37 °C, then mixed at a 10:1 ratio in fresh LB at a final OD_{600} of 0.33. Samples were plated onto selective media at 0 h to enumerate colony forming units (CFU) per mL for each population. The co-cultures were incubated at 37 °C with shaking for 4 h, then samples plated onto selective media to quantify viable target cell counts as CFU mL^{-1}.

Plasmid constructions

Super-folding *gfp* was amplified with primers gfp(mut3)-Bam-for/sfGFP-rev-Bam ligated into the BamHI site of plasmid pTrc99a. The *gfp* fragment was then subcloned into plasmid pCH450 using EcoRI and PstI restriction sites. The coding sequence for DsRed was amplified from plasmid DsRedExpress2 using primers dsRed-Eco-for/dsRed-Xho-rev and ligated into plasmid pCH450 using EcoRI and XhoI restriction sites. The coding sequence for the TPS transport domain of $CdiA^{EC93}$ was amplified using primers EC93cdiA-V33-Spe-for/EC93cdiA-G285-Xho-rev and ligated to plasmid pSH21P using SpeI and XhoI restriction sites. The resulting plasmid was used to over-produce N-terminal His_6-tagged TPS transport domain for purification and generation of polyclonal antibodies. Truncation and deletion mutations within cosmid-borne *cdiA* were generated using a series of plasmid

pDAL660Δ1-39 derivatives that carry random transprimer insertions as described (Aoki et al., 2005). Plasmids that carry in-frame stop codons after CdiA residues Val2905, Asn2556, Arg2123, Arg1930 and Arg1319 were used directly for cell-cell binding assays. In-frame deletions were created by digesting selected transprimer-containing plasmids with PmeI and SfiI, followed by re-ligation and transformation into EPI100 cells.

The IPTG-inducible *cdiBAI* expression plasmid was built in several steps. The *rrnB* transcription terminators from excised from plasmid pUC18T-miniTn7T-Kan (Choi *et al.*, 2008) with SacI/NheI and ligated to SacI/SpeI digested plasmid pKAN. The *lac* promoter was then amplified with primers lac-Sacfor/lac-OE-rev and the 5′-end of *cdiB* amplified with cdiB-OE-for/cdiB-Sac-rev. The two PCR products were combined using over-lapping end PCR (Aiyar *et al.*, 1996) with primers lac-Sac-for/cdiB-Sac-rev, and the fused product ligated to pKAN-*rrnB* using the SacI restriction site. The *lacI*^{q} gene was then amplified with primers lacI-Eco-for/lacI-Xho-rev and ligated using EcoRI and XhoI restriction sites. Finally, a fragment upstream of *cdiB* was amplified with primers CDI-up-Kpn-for/CDI-up-Xho-rev and ligated using XhoI and KpnI restriction sites. The final plasmid was amplified with primers CDI-up-Kpn-for/cdiB-Sac-rev and the resulting product was recombineered into plasmid pDAL660Δ1-39 to generate plasmid pCH12732.

Biofilm assays

Overnight cultures of *E. coli* EC93 and derivatives were inoculated into fresh tryptone broth supplemented with 0.5% glycerol at a final OD_{600} of 0.05. The cell suspension (200 μL) was added to the interior well(s) of a 96-well flat-bottom polystyrene plate and incubated at 37 °C for the indicated times. For proteinase K treated samples, 2 μL of 1 mg mL^{-1} proteinase K freshly dissolved in 1 × PBS was added to wells after 2 h of incubation. Suspended cells were removed by inversion of the plate followed by gentle tapping onto a clean paper towel. 200 μL of 0.1% crystal violet solution was added to sample wells and blank wells and incubated for 15 min at ambient temperature. The stain was removed by inversion of the plate and tapping onto a fresh paper towel. Wells were gently washed three times with 1 × PBS. Wells were destained with 0.2 mL of 95% ethanol followed by vigorous pipetting. Staining was quantified by measuring absorbance of the ethanol solution at 595 nm.

For confocal laser-scanning microscopic (CLSM) analysis of biofilms, overnight cultures of *E. coli* EC93 were diluted to OD_{600} of 0.02 in LB medium and 3 mL of the suspension inoculated into glass chambers (Lab-Tek) for incubation at 30 °C under static conditions. After 24 h, planktonic bacteria were removed by inverting the chambers and gentle washing with LB medium. Adherent cells were then stained with 1 μM SYTO-9 (Life Technologies) in the dark for 30 min. Biofilms were visualized with an LSM 5 Pascal laser-scanning microscope (Zeiss). Three-dimensional images were reconstructed using Imaris 7.6 and analyzed using COMSTAT (Heydorn *et al.*, 2000). Each experiment included 2 independent biological replicates, with three images taken for each replicate.

Gene expression analysis

E. coli EC93 biofilms were produced as described above. After incubation on polystyrene plates for 4 h, planktonic cells were gently removed with a pipette and the volume

immediately replaced with 200 μL of Qiagen RNA Protect Bacterial Reagent. Biofilms were harvested from the plate with rigorous pipeting and RNA extracted from the suspension using the Qiagen RNEasy kit with on-column DNase I digestion according to manufacturer's instructions. Total cDNA was prepared using the SuperScript III First Strand Synthesis kit. The relative abundance of *pgaA*, *wcaA*, *bcsA*, and *fliC* transcripts was determined by quantitative real-time PCR using primer pairs pgaA-for/pgaA-rev, wcaA-for/wcaA-rev, bcsA-for/bcsA-rev and fliC-for/fliC-rev, respectively with the SYBR Green Real-Time PCR Master Mix according to manufacturer's instructions. Comparative C_T analysis was performed as described (Schmittgen & Livak, 2008) using *pgaA* and *fliC* transcript levels as references.

Auto-aggregation assay

Strains CH9604 (*bamA*^{Eco}) and CH9591 (*bamA*^{ECL}) were transformed with IPTG-inducible CDI^{EC93} system plasmid and tested for auto-aggregation upon induction. Cells were grown to OD_{600} ~1.0 in TB supplemented with 0.5% glycerol with or without 1.5 mM IPTG. Cells were harvested and resuspended in 20 mL of spent media at OD_{600} ~ 0.6 – 0.7. The resuspended cells were transferred to a 13 cm glass culture tube and incubated at 37 °C without agitation. The OD_{600} was measured at the top of the cell suspension at 30, 60, 120 and 240 min. BamA^{Eco} independent auto-aggregation was determined in the same manner for CdiA^{EC93} truncation and deletion variants expressed in strain CH9591 (*bamA*^{ECL}), except no IPTG induction was required to express these proteins.

Flow cytometry

BamA^{Eco} receptor binding studies were conducted using strain DL4259, which expresses *gfp-mut3* from the *papIB* promoter (Webb *et al.*, 2013). DL4259 was transformed with cosmids that express CdiA^{EC93} truncation and deletion variants, then grown in LB medium supplemented with ampicillin in baffled flasks at 37 °C until the cells became fluorescent. Fluorescent DL4259 cells were mixed at a 5:1 ratio with DsRed-expressing CH9604 (*bamA*^{Eco}) or CH9591 (*bamA*^{ECL}) cells at a final OD_{600} of 0.2. the cell suspension were shaken at 30 °C for 20 min, diluted into 1 × PBS, vortexed briefly, then analyzed on an Accuri C6 flow cytometer using FL1 (533/30nm, GFP) and FL2 (585/40nm, DsRed) fluorophore filters. Percent target-cell binding was calculated as the number of dual green/red fluorescent events divided by the total number of red fluorescent events (Ruhe et al., 2013b).

For receptor-independent binding assays, CH9591 (*bamA*^{ECL}) cells harboring pWEB-TNC (CDI^{-}) or pDAL660Δ1-39 (CDI^{+}) were labeled with GFP (pCH450::sfGFP) or DsRed (pCH450::DsRed), and the green- and red-labeled populations were mixed at a 1:1 ratio in 0.55 LB medium supplemented with ampicillin, tetracycline and 0.2% arabinose. Cell mixtures were grown with shaking at 37 °C until the cells became fluorescent, then the cultures were diluted into 1 × PBS, vortexed briefly and analyzed by flow cytometry. Forward-scatter analyses were performed on strains CH9604 (*bamA*^{Eco}) and CH9591 (*bamA*^{ECL}) that carry CDI expression cosmids. Overnight cultures were diluted 1:100 in fresh LB media supplemented with ampicillin and grown with shaking for 4 h at 37 °C.

Cells were diluted into 1 × PBS, mixed gently, and analyzed by flow cytometry for forward scatter and by light microscopy to visualize cell aggregates.

CdiA^{EC93} TPS transport domain purification

The His_6-tagged TPS transport domain (CdiA^{EC93} residues Val33 – Gly285) was overproduced in *E. coli* strain CH2016 harboring plasmid pSH21P*::cdiA(V33-G285)*. An overnight culture was diluted 1:100 in fresh LB supplemented with ampicillin and grown to mid-log phase at 37 °C in a baffled flask. Expression was then induced with the addition of 1.5 mM IPTG for 90 min. Cells were harvested by centrifugation and the pellet was frozen at −80°C. Cells were broken by freeze-thaw in urea lysis buffer (8 M urea, 150 mM NaCl, 0.05% Triton X-100, and 20 mM imidazole) as described previously (Garza-Sánchez *et al.*, 2006). The CdiA^{EC93} TPS domain was purified via Ni^{2+}-affinity chromatography under denaturing conditions in urea lysis buffer, followed by elution in urea lysis buffer supplemented with 25 mM EDTA. The purified TPS domain was judged to be >95% pure by SDS-PAGE analysis and was used to generate rabbit polyclonal antibodies (Cocalico Biologicals Inc., Reamstown, PA).

Proteinase K treatment and immunoblot analysis

Overnight cultures of strain CH9591 (*bamA*^{ECL}) carrying CDI cosmids were diluted 1:100 into 2 mL fresh LB without antibiotics and grown at 37 °C to OD_{600} ~1.0. Cells were harvested, resuspended in 2 mL of 1 × PBS, and split into two 1 mL aliquots. 100 μg mL^{-1} proteinase K (final concentration) or buffer was added to each cell aliquot followed by incubation at 37°C for 1 h. Cells were harvested and resuspended in 1 mL 1 × PBS, 1 mM freshly prepared phenylmethylsulfonyl fluoride (PMSF). Cells were harvested by centrifugation and washed three times with 1 mL 1 × PBS supplemented with 1 mM PMSF. Washed cells were broken by freeze-thaw lysis in 75 μL of urea lysis buffer, 1 mM PMSF. Urea lysates (50 μg total protein) were run on SDS-6% polyacrylamide gels and blotted onto nitrocellulose for immunoblot analysis using polyclonal antibodies to the N-terminal TPS transport domain of CdiA^{EC93}. Blots were visualized using IRDye® 680 (LI-COR) labeled anti-rabbit secondary antibodies and an Odyssey® infrared imager.

Supplementary Material

Refer to Web version on PubMed Central for supplementary material.

Acknowledgments

Z.C.R. was supported by the Tri-Counties Blood Bank Postdoctoral Fellowship. This work was supported by grants AI114261 (F.H.Y.) and GM102318 (D.A.L & C.S.H.) from the National Institutes of Health.

References

Aiyar A, Xiang Y, Leis J. Site-directed mutagenesis using overlap extension PCR. Methods Mol Biol. 1996; 57:177–191. [PubMed: 8850005]

Anderson MS, Garcia EC, Cotter PA. The *Burkholderia bcpAIOB* genes define unique classes of two-partner secretion and contact dependent growth inhibition systems. PLoS Genet. 2012; 8:e1002877. [PubMed: 22912595]

Anderson MS, Garcia EC, Cotter PA. Kind discrimination and competitive exclusion mediated by contact-dependent growth inhibition systems shape biofilm community structure. PLoS Pathog. 2014; 10:e1004076. [PubMed: 24743836]

Aoki SK, Diner EJ, de Roodenbeke CT, Burgess BR, Poole SJ, Braaten BA, Jones AM, Webb JS, Hayes CS, Cotter PA, Low DA. A widespread family of polymorphic contact-dependent toxin delivery systems in bacteria. Nature. 2010; 468:439–442. [PubMed: 21085179]

Aoki SK, Malinverni JC, Jacoby K, Thomas B, Pamma R, Trinh BN, Remers S, Webb J, Braaten BA, Silhavy TJ, Low DA. Contact-dependent growth inhibition requires the essential outer membrane protein BamA (YaeT) as the receptor and the inner membrane transport protein AcrB. Mol Microbiol. 2008; 70:323–340. [PubMed: 18761695]

Aoki SK, Pamma R, Hernday AD, Bickham JE, Braaten BA, Low DA. Contact- dependent inhibition of growth in *Escherichia coli*. Science. 2005; 309:1245–1248. [PubMed: 16109881]

Aoki SK, Webb JS, Braaten BA, Low DA. Contact-dependent growth inhibition causes reversible metabolic downregulation in *Escherichia coli*. J Bacteriol. 2009; 191:1777–1786. [PubMed: 19124575]

Arenas J, Schipper K, van Ulsen P, van der Ende A, Tommassen J. Domain exchange at the 3′ end of the gene encoding the fratricide meningococcal two-partner secretion protein A. BMC Genomics. 2013; 14:622. [PubMed: 24034852]

Balder R, Hassel J, Lipski S, Lafontaine ER. *Moraxella catarrhalis* strain O35E expresses two filamentous hemagglutinin-like proteins that mediate adherence to human epithelial cells. Infect Immun. 2007; 75:2765–2775. [PubMed: 17371858]

Baud C, Guerin J, Petit E, Lesne E, Dupre E, Locht C, Jacob-Dubuisson F. Translocation path of a substrate protein through its Omp85 transporter. Nat Commun. 2014; 5:5271. [PubMed: 25327833]

Beck CM, Morse RP, Cunningham DA, Iniguez A, Low DA, Goulding CW, Hayes CS. CdiA from *Enterobacter cloacae* delivers a toxic ribosomal RNase into target bacteria. Structure. 2014; 22:707–718. [PubMed: 24657090]

Beckwith JR, Signer ER. Transposition of the lac region of *Escherichia coli*. I. Inversion of the lac operon and transduction of lac by phi80. J Mol Biol. 1966; 19:254–265. [PubMed: 5338856]

Cherepanov PP, Wackernagel W. Gene disruption in *Escherichia coli*: TcR and KmR cassettes with the option of Flp-catalyzed excision of the antibiotic-resistance determinant. Gene. 1995; 158:9–14. [PubMed: 7789817]

Choi KH, Mima T, Casart Y, Rholl D, Kumar A, Beacham IR, Schweizer HP. Genetic tools for select-agent-compliant manipulation of *Burkholderia pseudomallei*. Appl Environ Microbiol. 2008; 74:1064–1075. [PubMed: 18156318]

Danese PN, Pratt LA, Kolter R. Exopolysaccharide production is required for development of *Escherichia coli* K-12 biofilm architecture. J Bacteriol. 2000; 182:3593–3596. [PubMed: 10852895]

Datta S, Costantino N, Court DL. A set of recombineering plasmids for gram-negative bacteria. Gene. 2006; 379:109–115. [PubMed: 16750601]

Dawkins, R. The Selfish Gene. Oxford Univ. Press; Oxford: 1976. p. 224

Diner EJ, Beck CM, Webb JS, Low DA, Hayes CS. Identification of a target cell permissive factor required for contact-dependent growth inhibition (CDI). Genes Dev. 2012; 26:515–525. [PubMed: 22333533]

Dobrindt U, Blum-Oehler G, Nagy G, Schneider G, Johann A, Gottschalk G, Hacker J. Genetic structure and distribution of four pathogenicity islands (PAI I(536) to PAI IV(536)) of uropathogenic Escherichia coli strain 536. Infect Immun. 2002; 70:6365–6372. [PubMed: 12379716]

Doerrler WT, Raetz CR. Loss of outer membrane proteins without inhibition of lipid export in an *Escherichia coli* YaeT mutant. J Biol Chem. 2005; 280:27679–27687. [PubMed: 15951436]

Garcia EC, Anderson MS, Hagar JA, Cotter PA. *Burkholderia BcpA* mediates biofilm formation independently of interbacterial contact-dependent growth inhibition. Mol Microbiol. 2013

Garza-Sánchez F, Janssen BD, Hayes CS. Prolyl-tRNA^{Pro} in the A-site of SecM-arrested ribosomes inhibits the recruitment of transfer-messenger RNA. J Biol Chem. 2006; 281:34258–34268. [PubMed: 16968693]

Girard V, Cote JP, Charbonneau ME, Campos M, Berthiaume F, Hancock MA, Siddiqui N, Mourez M. Conformation change in a self-recognizing autotransporter modulates bacterial cell-cell interaction. J Biol Chem. 2010; 285:10616–10626. [PubMed: 20123991]

Gottig N, Garavaglia BS, Garofalo CG, Orellano EG, Ottado J. A filamentous hemagglutinin-like protein of *Xanthomonas axonopodis* pv. citri, the phytopathogen responsible for citrus canker, is involved in bacterial virulence. PLoS One. 2009; 4:e4358. [PubMed: 19194503]

Guilhabert MR, Kirkpatrick BC. Identification of Xylella fastidiosa antivirulence genes: hemagglutinin adhesins contribute X. fastidiosa biofilm maturation and colonization and attenuate virulence. Mol Plant Microbe Interact. 2005; 18:856–868. [PubMed: 16134898]

Hayes CS, Aoki SK, Low DA. Bacterial contact-dependent delivery systems. Annu Rev Genet. 2010; 44:71–90. [PubMed: 21047256]

Hayes CS, Bose B, Sauer RT. Proline residues at the C terminus of nascent chains induce SsrA tagging during translation termination. J Biol Chem. 2002; 277:33825–33832. [PubMed: 12105207]

Hayes CS, Koskiniemi S, Ruhe ZC, Poole SJ, Low DA. Mechanisms and biological roles of contact-dependent growth inhibition systems. Cold Spring Harb Perspect Med. 2014; 4

Hayes CS, Sauer RT. Cleavage of the A site mRNA codon during ribosome pausing provides a mechanism for translational quality control. Mol. Cell. 2003; 12:903–911. [PubMed: 14580341]

Heydorn A, Nielsen AT, Hentzer M, Sternberg C, Givskov M, Ersboll BK, Molin S. Quantification of biofilm structures by the novel computer program COMSTAT. Microbiology. 2000; 146(Pt 10): 2395–2407. [PubMed: 11021916]

Irie Y, Mattoo S, Yuk MH. The Bvg virulence control system regulates biofilm formation in Bordetella bronchiseptica. J Bacteriol. 2004; 186:5692–5698. [PubMed: 15317773]

Ishibashi Y, Claus S, Relman DA. Bordetella pertussis filamentous hemagglutinin interacts with a leukocyte signal transduction complex and stimulates bacterial adherence to monocyte CR3 (CD11b/CD18). J Exp Med. 1994; 180:1225–1233. [PubMed: 7931059]

Itoh Y, Wang X, Hinnebusch BJ, Preston JF 3rd, Romeo T. Depolymerization of beta- 1,6-N-acetyl-D-glucosamine disrupts the integrity of diverse bacterial biofilms. J Bacteriol. 2005; 187:382–387. [PubMed: 15601723]

Jacob-Dubuisson F, Guerin J, Baelen S, Clantin B. Two-partner secretion: as simple as it sounds? Res Microbiol. 2013; 164:583–595. [PubMed: 23542425]

Jensen RB, Gerdes K. Programmed cell death in bacteria: proteic plasmid stabilization systems. Mol Microbiol. 1995; 17:205–210. [PubMed: 7494469]

Kajava AV, Cheng N, Cleaver R, Kessel M, Simon MN, Willery E, Jacob-Dubuisson F, Locht C, Steven AC. Beta-helix model for the filamentous haemagglutinin adhesin of Bordetella pertussis and related bacterial secretory proteins. Mol Microbiol. 2001; 42:279–292. [PubMed: 11703654]

Kim S, Malinverni JC, Sliz P, Silhavy TJ, Harrison SC, Kahne D. Structure and function of an essential component of the outer membrane protein assembly machine. Science. 2007; 317:961–964. [PubMed: 17702946]

Koskiniemi S, Garza-Sanchez F, Edman N, Chaudhuri S, Poole SJ, Manoil C, Hayes CS, Low DA. Genetic analysis of the CDI Pathway from *Burkholderia pseudomallei* 1026b. PLoS One. 2015; 10:e0120265. [PubMed: 25786241]

Koskiniemi S, Garza-Sanchez F, Sandegren L, Webb JS, Braaten BA, Poole SJ, Andersson DI, Hayes CS, Low DA. Selection of orphan Rhs toxin expression in evolved Salmonella enterica serovar Typhimurium. PLoS Genet. 2014; 10:e1004255. [PubMed: 24675981]

Locht C, Bertin P, Menozzi FD, Renauld G. The filamentous haemagglutinin, a multifaceted adhesion produced by virulent Bordetella spp. Mol Microbiol. 1993; 9:653–660. [PubMed: 8231801]

Lutz R, Bujard H. Independent and tight regulation of transcriptional units in *Escherichia coli* via the LacR/O, the TetR/O and AraC/I1-I2 regulatory elements. Nucleic Acids Res. 1997; 25:1203–1210. [PubMed: 9092630]

Majerczyk C, Brittnacher M, Jacobs M, Armour CD, Radey M, Schneider E, Phattarasokul S, Bunt R, Greenberg EP. Global analysis of the *Burkholderia thailandensis* quorum sensing-controlled regulon. J Bacteriol. 2014; 196:1412–1424. [PubMed: 24464461]

Menozzi FD, Boucher PE, Riveau G, Gantiez C, Locht C. Surface-associated filamentous hemagglutinin induces autoagglutination of Bordetella pertussis. Infect Immun. 1994; 62:4261–4269. [PubMed: 7927683]

Morse RP, Nikolakakis KC, Willett JL, Gerrick E, Low DA, Hayes CS, Goulding CW. Structural basis of toxicity and immunity in contact-dependent growth inhibition (CDI) systems. Proc Natl Acad Sci U S A. 2012; 109:21480–21485. [PubMed: 23236156]

Neil RB, Apicella MA. Role of HrpA in biofilm formation of Neisseria meningitidis and regulation of the hrpBAS transcripts. Infect Immun. 2009; 77:2285–2293. [PubMed: 19289515]

Nikolakakis K, Amber S, Wilbur JS, Diner EJ, Aoki SK, Poole SJ, Tuanyok A, Keim PS, Peacock S, Hayes CS, Low DA. The toxin/immunity network of *Burkholderia pseudomallei* contact-dependent growth inhibition (CDI) systems. Mol Microbiol. 2012; 84:516–529. [PubMed: 22435733]

Poole SJ, Diner EJ, Aoki SK, Braaten BA, t'Kint de Roodenbeke C, Low DA, Hayes CS. Identification of functional toxin/immunity genes linked to contact-dependent growth inhibition (CDI) and rearrangement hotspot (Rhs) systems. PLoS Genet. 2011; 7:e1002217. [PubMed: 21829394]

Prigent-Combaret C, Vidal O, Dorel C, Lejeune P. Abiotic surface sensing and biofilm- dependent regulation of gene expression in *Escherichia coli*. J Bacteriol. 1999; 181:5993–6002. [PubMed: 10498711]

Relman D, Tuomanen E, Falkow S, Golenbock DT, Saukkonen K, Wright SD. Recognition of a bacterial adhesion by an integrin: macrophage CR3 (alpha M beta 2, CD11b/CD18) binds filamentous hemagglutinin of Bordetella pertussis. Cell. 1990; 61:1375–1382. [PubMed: 2364431]

Rojas CM, Ham JH, Deng WL, Doyle JJ, Collmer A. HecA, a member of a class of adhesins produced by diverse pathogenic bacteria, contributes to the attachment, aggregation, epidermal cell killing, and virulence phenotypes of Erwinia chrysanthemi EC16 on Nicotiana clevelandii seedlings. Proc Natl Acad Sci U S A. 2002; 99:13142–13147. [PubMed: 12271135]

Ruhe ZC, Low DA, Hayes CS. Bacterial contact-dependent growth inhibition. Trends Microbiol. 2013a; 21:230–237. [PubMed: 23473845]

Ruhe ZC, Nguyen JY, Beck CM, Low DA, Hayes CS. The proton-motive force is required for translocation of CDI toxins across the inner membrane of target bacteria. Mol Microbiol. 2014; 94:466–481. [PubMed: 25174572]

Ruhe ZC, Wallace AB, Low DA, Hayes CS. Receptor polymorphism restricts contact- dependent growth inhibition to members of the same species. mBio. 2013b; 4:e00480–00413. [PubMed: 23882017]

Schmitt C, Turner D, Boesl M, Abele M, Frosch M, Kurzai O. A functional two-partner secretion system contributes to adhesion of Neisseria meningitidis to epithelial cells. J Bacteriol. 2007; 189:7968–7976. [PubMed: 17873034]

Schmittgen TD, Livak KJ. Analyzing real-time PCR data by the comparative C(T) method. Nat Protoc. 2008; 3:1101–1108. [PubMed: 18546601]

Serra DO, Conover MS, Arnal L, Sloan GP, Rodriguez ME, Yantorno OM, Deora R. FHA-mediated cell-substrate and cell-cell adhesions are critical for Bordetella pertussis biofilm formation on abiotic surfaces and in the mouse nose and the trachea. PLoS One. 2011; 6:e28811. [PubMed: 22216115]

Serra DO, Richter AM, Hengge R. Cellulose as an architectural element in spatially structured *Escherichia coli* biofilms. J Bacteriol. 2013; 195:5540–5554. [PubMed: 24097954]

Smith DL, James CE, Sergeant MJ, Yaxian Y, Saunders JR, McCarthy AJ, Allison HE. Short-tailed stx phages exploit the conserved YaeT protein to disseminate Shiga toxin genes among enterobacteria. J Bacteriol. 2007; 189:7223–7233. [PubMed: 17693515]

Strassmann JE, Gilbert OM, Queller DC. Kin discrimination and cooperation in microbes. Annu Rev Microbiol. 2011; 65:349–367. [PubMed: 21682642]

Tala A, Progida C, De Stefano M, Cogli L, Spinosa MR, Bucci C, Alifano P. The HrpB HrpA two-partner secretion system is essential for intracellular survival of Neisseria meningitidis. Cell Microbiol. 2008; 10:2461–2482. [PubMed: 18680551]

Thomason L, Court DL, Bubunenko M, Costantino N, Wilson H, Datta S, Oppenheim A. Recombineering: genetic engineering in bacteria using homologous recombination. Current protocols in molecular biology / edited by Frederick M. Ausubel. 2007 [et al Chapter 1: Unit 1 16.

Voulhoux R, Bos MP, Geurtsen J, Mols M, Tommassen J. Role of a highly conserved bacterial protein in outer membrane protein assembly. Science. 2003; 299:262–265. [PubMed: 12522254]

Walker D, Lancaster L, James R, Kleanthous C. Identification of the catalytic motif of the microbial ribosome inactivating cytotoxin colicin E3. Protein Sci. 2004; 13:1603–1611. [PubMed: 15133158]

Wang X, Preston JF 3rd, Romeo T. The pgaABCD locus of *Escherichia coli* promotes the synthesis of a polysaccharide adhesin required for biofilm formation. J Bacteriol. 2004; 186:2724–2734. [PubMed: 15090514]

Webb JS, Nikolakakis KC, Willett JL, Aoki SK, Hayes CS, Low DA. Delivery of CdiA nuclease toxins into target cells during contact-dependent growth inhibition. PLoS ONE. 2013; 8:e57609. [PubMed: 23469034]

Werner J, Misra R. YaeT (Omp85) affects the assembly of lipid-dependent and lipid-independent outer membrane proteins of *Escherichia coli*. Mol Microbiol. 2005; 57:1450–1459. [PubMed: 16102012]

West SA, Gardner A. Altruism, spite, and greenbeards. Science. 2010; 327:1341–1344. [PubMed: 20223978]

Wozniak RA, Waldor MK. A toxin-antitoxin system promotes the maintenance of an integrative conjugative element. PLoS Genet. 2009; 5:e1000439. [PubMed: 19325886]

Wu T, Malinverni J, Ruiz N, Kim S, Silhavy TJ, Kahne D. Identification of a multicomponent complex required for outer membrane biogenesis in *Escherichia coli*. Cell. 2005; 121:235–245. [PubMed: 15851030]

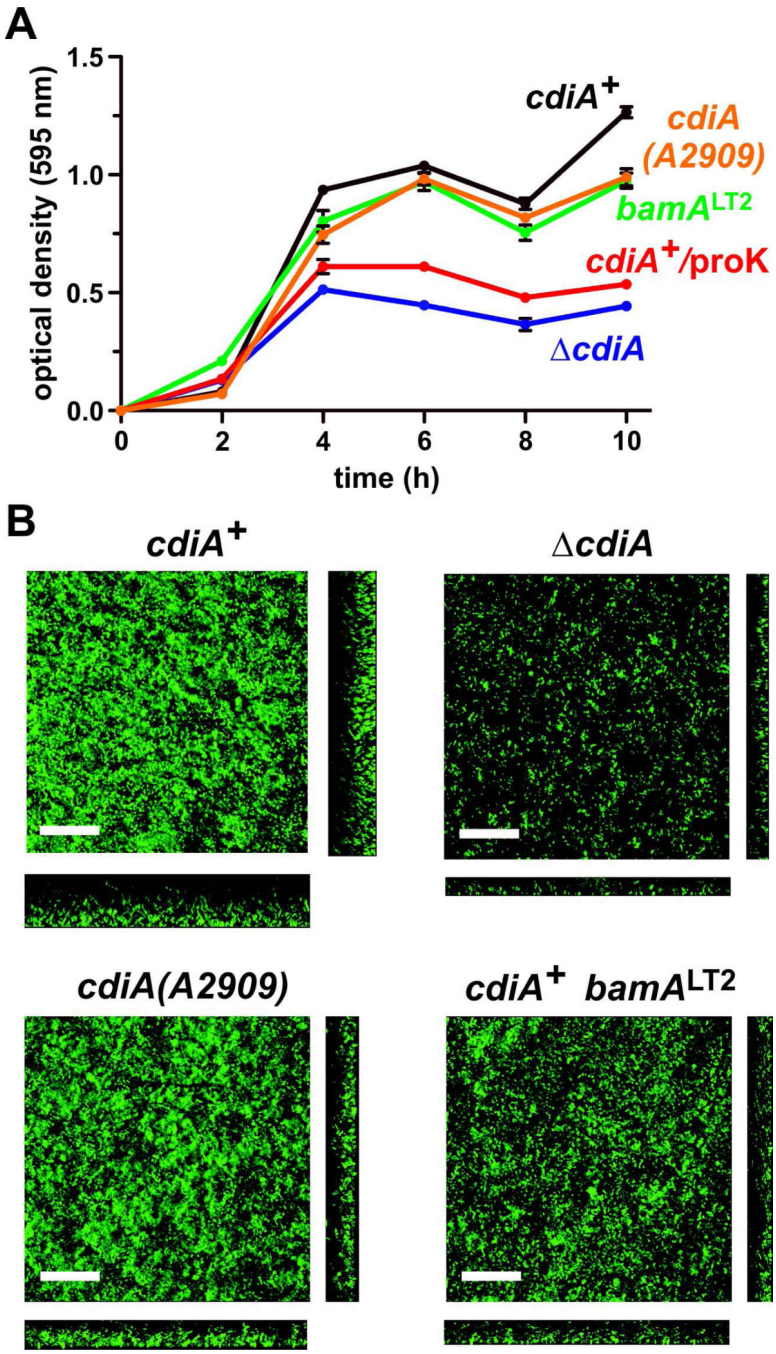

Figure 1. *E. coli* EC93 Δ*cdiA* mutants are defective for biofilm formation

A) Crystal violet staining of biofilms grown in polystyrene wells. The indicated strains of *E. coli* EC93 were grown in 96-well plates as described in the Methods. Planktonic cells were removed and the adherent biofilms stained with crystal violet. Staining was quantified by measuring the optical density at 595 nm (OD_{595}). Where indicated, proteinase K was added to wild-type *E. coli* EC93 cultures after 2 h to determine the role of extracellular protein in biofilm formation. Each strain was tested in triplicate in two independent experiments. Presented values are the average ± SEM. **B**) Three-dimensional biofilm structures of *E. coli*

EC93 strains after 24 h incubation in static biofilm chambers. Horizontal (*xy*) and vertical (*xz*) projections of biofilms are shown. Representative images are shown from one of two independent experiments. Inset scale bars equal 40 μm.

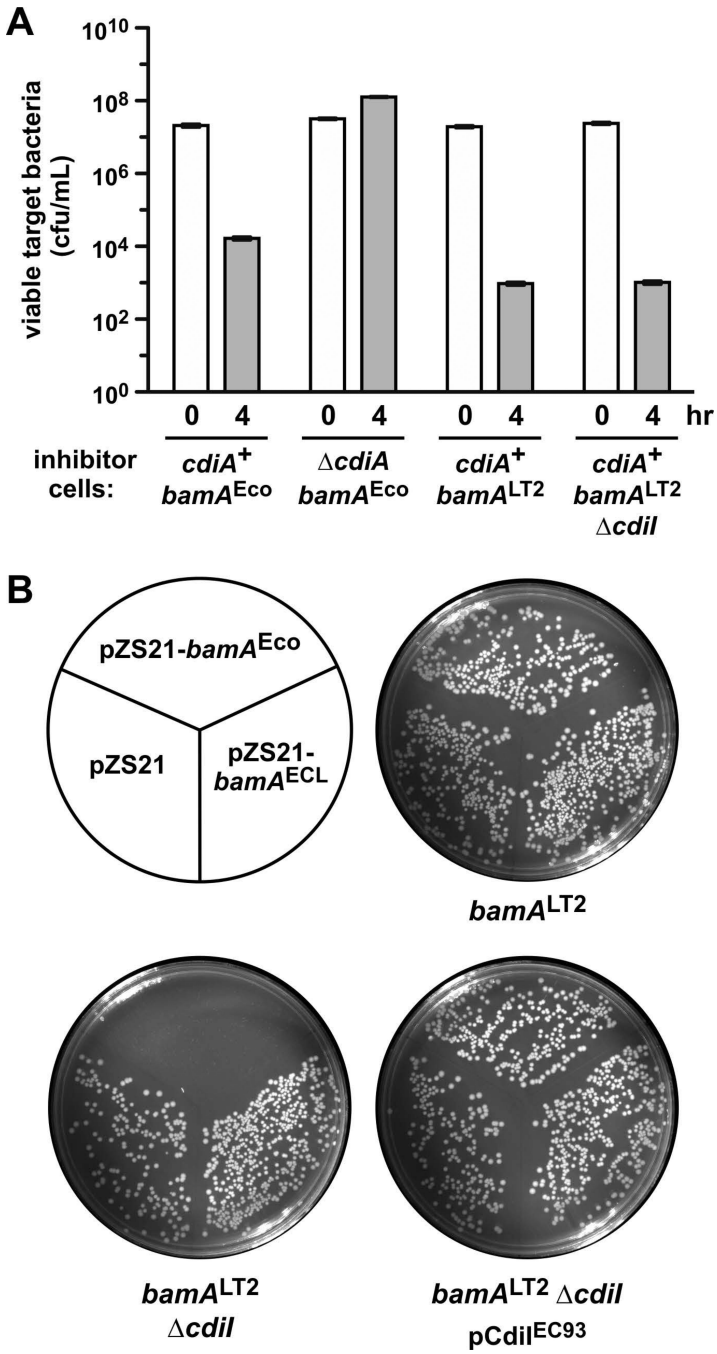

Figure 2. *E. coli* EC93 *bamA*^{LT2} cells retain the CDI^{+} inhibitor cell phenotype

A) *E. coli* EC93 strains of the indicated genotype were used as inhibitor cells in competition co-cultures with *E. coli* X90 target bacteria. Viable target bacteria were enumerated as colony forming units per mL at 0 and 4 h. The mean ± SEM is presented for two independent competition experiments. **B**) The *cdiI* immunity gene can be deleted from *E. coli* EC93 *bamA*^{LT2} cells. Strains CH10060 (*bamA*^{LT2}), CH10151 (*bamA*^{LT2} Δ*cdiI*) and CH10151 carrying pDAL741 (*cdiI*$^{+}$) were transformed with the indicated plasmids that

express *bamA*^{Eco} or *bamA*^{ECL}, followed by plating onto LB agar supplemented with kanamycin.

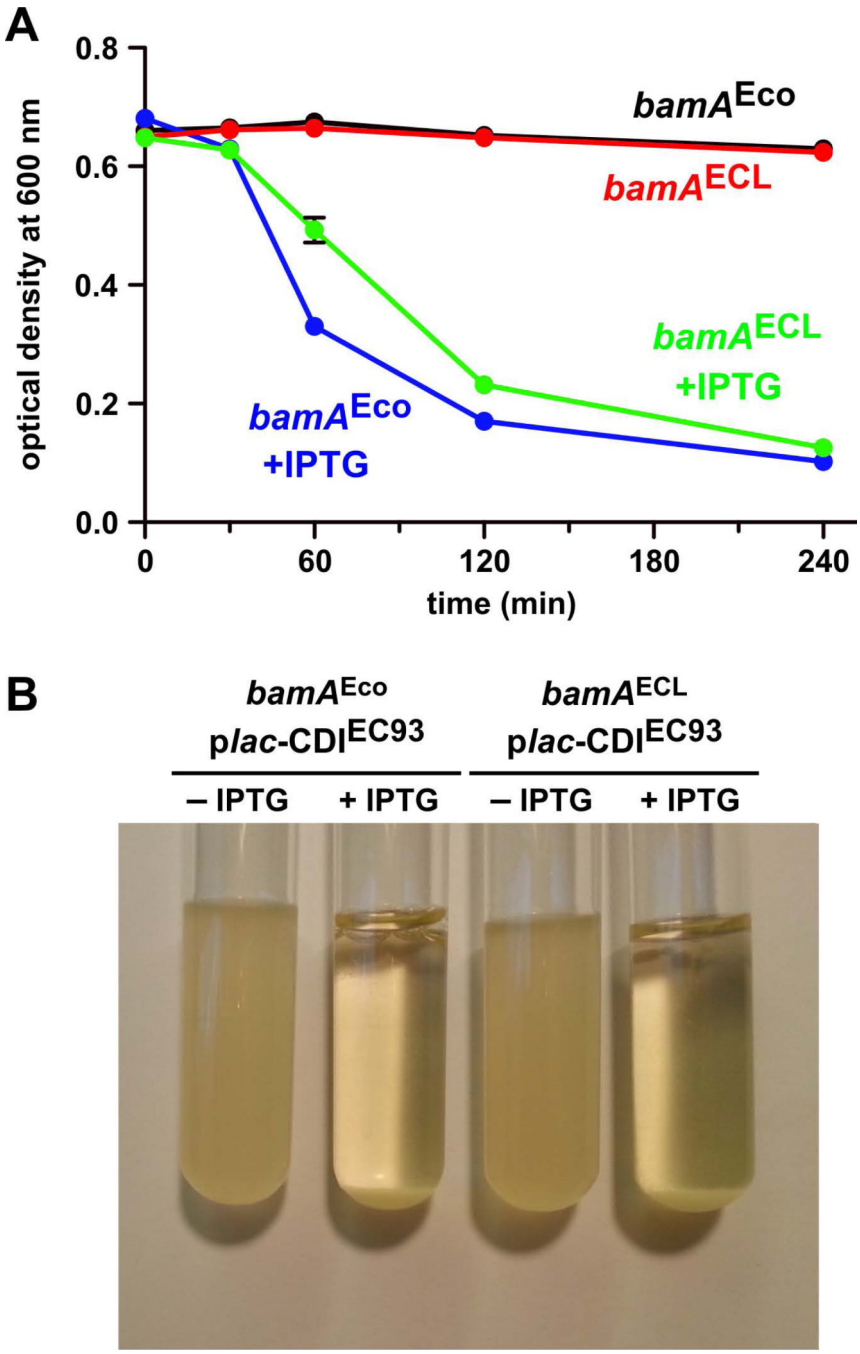

Figure 3. Expression of the *cdiBAI*^{EC93} gene cluster induces auto-aggregation

A) Strains CH9604 (*bamA*^{Eco}) and CH9591 (*bamA*^{ECL}) that carry plasmid pCH12732 were grown in LB medium with and without IPTG, then adjusted to OD_{600} ~ 0.6 for auto-aggregation assays. **B**) Photograph of the cell suspensions from panel A after four h of incubation without shaking.

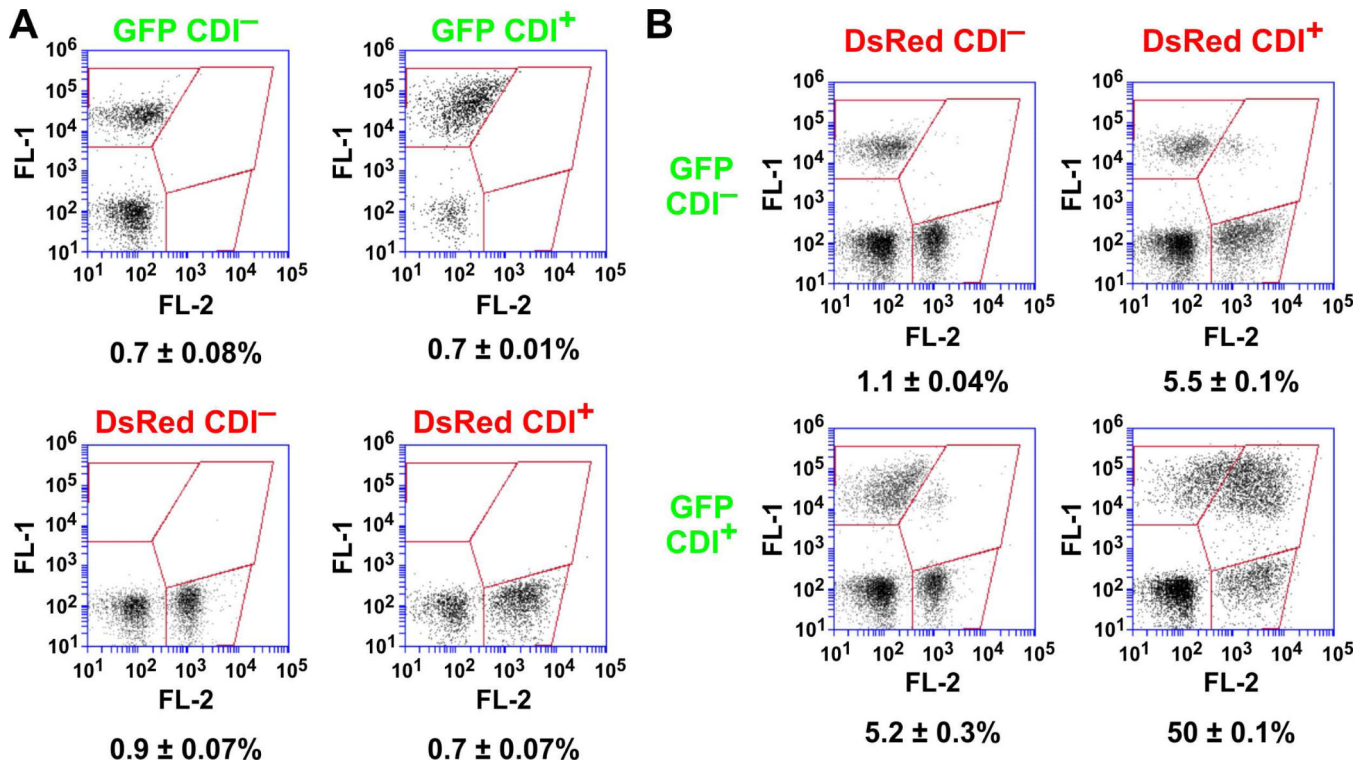

Figure 4. CDI expression is required for auto-aggregation

A) CH9591 (*bamA*^{ECL}) cells were transformed with pTNC-WEB (CDI^{-}) or pDAL660Δ1-39 (CDI^{+}) plasmids and labeled with GFP or DsRed. Each of the four cell populations was analyzed by flow cytometry to detect background levels of dual green/red fluorescent events. **B**) The individual cell populations show in panel **A** were mixed at 1:1 ratio and incubated with shaking at 37 °C. The suspensions were then analyzed by flow cytometry using FL1 (533/30nm, GFP) and FL2 (585/40nm, DsRed) fluorophore filters.

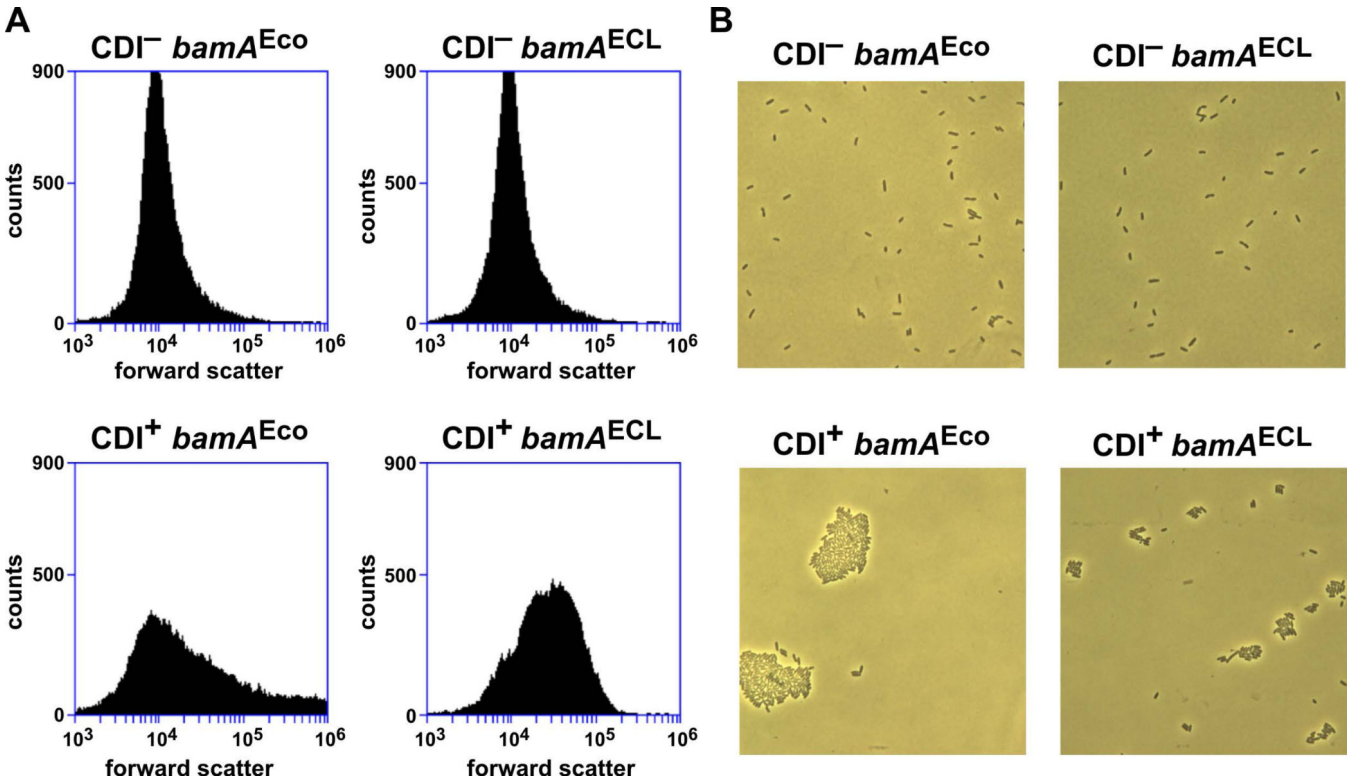

Figure 5. Flow cytometric and microscopic analysis of CDI-dependent aggregates

A) Strains CH9604 (*bamA*^{Eco}) and CH9591 (*bamA*^{ECL}) that carry either pTNC-WEB (CDI^{-}) or pDAL660Δ1-39 (CDI^{+}) were grown in LB medium and analyzed by flow cytometry for forward scatter. **B**) The cells from prepared for panel **A** were also visualized by light microscopy to determine the number of bacterial cells per aggregate.

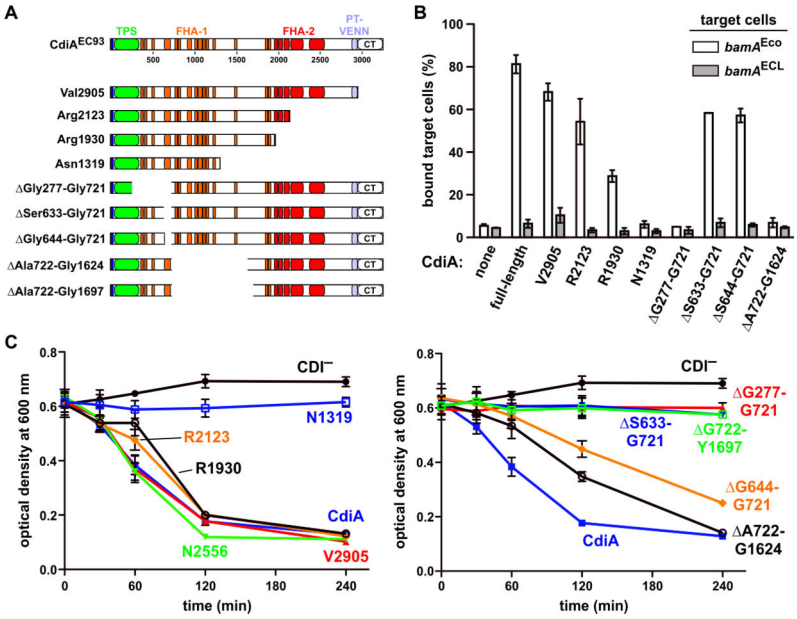

Figure 6. Receptor-dependent and -independent adhesion domains map to distinct positions within CdiA^{EC93}

A) Architecture of CdiA^{EC93}. The CdiA^{EC93} is composed of an N-terminal TPS transport domain (green) followed by two distinct regions of filamentous hemagglutinin peptide repeats (FHA-1 and FHA-2). The pretoxin-VENN (PT-VENN) domain demarcates the C-terminal toxin region. The various CdiA^{EC93} truncations and in-frame deletions are shown schematically. **B**) BamA^{Eco}-dependent target-cell binding assays. DL4259 cells that carry pTNC-WEB (none) or the indicated CDI cosmids were mixed at a 5:1 ratio with CH9604 (*bamA*^{Eco}) and CH9591 (*bamA*^{ECL}) target cells that express DsRed. The suspensions were analyzed by flow cytometry using FL1 (533/30nm, GFP) and FL2 (585/40nm, DsRed) fluorophore filters. The percentage of bound target cells was calculated as the number of dual green/red fluorescent events divided by the total number of red fluorescent events. The average ± SEM is presented for two independent cell-binding experiments. **C**) Auto-aggregation of CdiA^{EC93} mutants. Mono-cultures of *E. coli* CH9591 (*bamA*^{ECL}) that express the indicated CdiA^{EC93} truncation and in-frame deletion variants were suspended and allowed to sediment at 1 × *g* to monitor auto-aggregation.

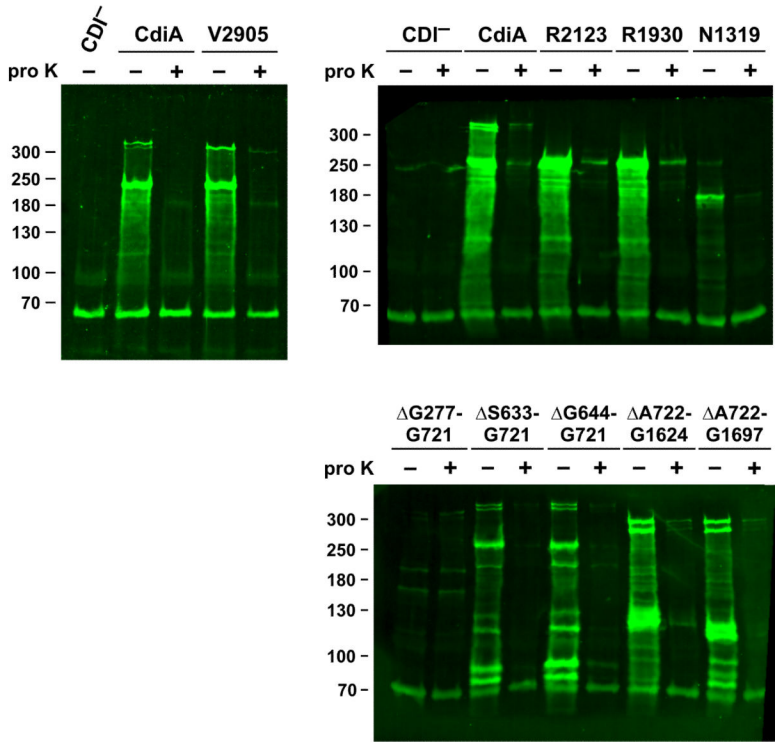

Figure 7. Immunoblot analysis of CdiA^{EC93} truncation and deletion variants

CH9591 (*bamA*^{ECL}) cells that produce the indicated CdiA^{EC93} proteins were treated with 100 μg mL^{-1} of extracellular proteinase K (proK) where indicated. Proteinase K digestion was quenched with 1 mM PMSF and total urea-soluble protein was extracted. Proteins were resolved on SDS 6% polyacrylamide gels and transferred to nitrocellulose for immunoblot analysis using polyclonal antibodies to the CdiA^{EC93} TPS domain. The migration position of molecular weight standards are indicated in kDa. The predicted mass of full-length CdiA^{EC93} is ~319 kDa.

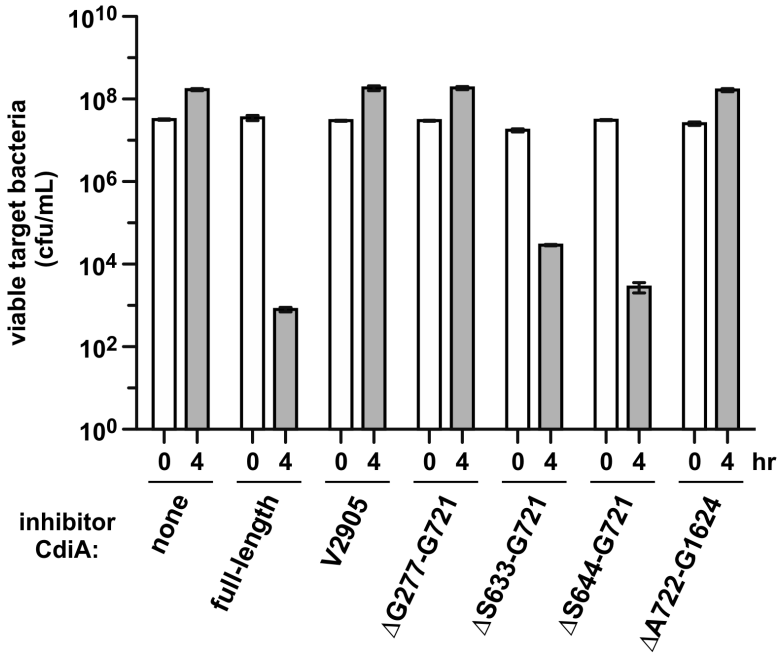

Figure 8. Competition co-cultures with CdiA^{EC93} truncation and deletion variants

Stain CH9591 (*bamA*^{ECL}) cells that express the indicated CdiA^{EC93} variants were used as inhibitor cells in competition co-cultures with *E. coli* X90 target cells. Inhibitors were mixed at a 10:1 ratio with targets and incubated with shaking at 37 °C for four h. Viable target bacteria were enumerated as colony forming units per mL and counts are presented as the average ± SEM for two independent experiments.

Table 1

COMSTAT analysis of *E. coli* EC93 biofilms[a]

Strain genotype	Biomass ($\mu m^3\ \mu m^{-2}$)	Average thickness (μm)	Maximum thickness (μm)	Roughness coefficient
cdiA$^+$	3.71 (0.42)	9.23 (0.08)	30.54 (2.02)	0.57 (0.03)
Δ *cdiA*	0.92 (0.01)	0.09 (0.00)	18.92 (0.44)	1.98 (0.00)
cdiA(A2909)	2.38 (0.09)	7.58 (2.22)	27.72 (1.32)	0.96 (0.18)
cdiA$^+$ *bamA* ^{LT2}	1.48 (0.11)	3.69 (2.38)	23.76 (0.00)	1.37 (0.35)

[a]Values represent the average ± SEM from two independent experiments

Table 2

Bacterial strains

Strains	***Description*** [a]	***Reference***
X90	F′ *lacI*^{q} *lac′pro′/ara* Δ*(lac-pro) nal1 argE*(amb) *rif*^{r} *thi-1*, Rif^{R}	(Beckwith & Signer, 1966)
EPI100	F^{-} *mcrA* Δ*(mrr-hsdRMS-mcrBC) ϕ80dlacZΔM15* Δ*lacXcZΔM15* Δ*lacX recA1 endA1 araD139* Δ*(ara, leu)7697 galU galK* ⁄$^{-}$ *rpsL nupG*, Str^{R}	Epicentre
DY378	W3110 λ*cI857* Δ*(cro-bioA)*	(Thomason et al., 2007)
EC93	*Escherichia coli* isolate from rat feces	(Aoki et al., 2005)
DL4259	*E. coli* MC4100 that expresses GFP-mut3	(Morse et al., 2012)
CH2016	X90 (DE3) Δ*rna* Δ*slyD::kan*, Rif^{R} Kan^{R}	(Garza-Sánchez et al., 2006)
CH9350	X90 Δ*bamA::cat* pZS21-*bamA*$^{+}$, Cm^{R} Kan^{R}	(Ruhe et al., 2013b)
CH9371	X90 Δ*bamA::cat* pZS21-*bamA*^{ECL}, Cm^{R} Kan^{R}	(Ruhe et al., 2013b)
CH9591	EPI100 Δ*bamA::cat* pZS21-*bamA*^{ECL}, Cm^{R} Kan^{R}	(Ruhe et al., 2013b)
CH9604	EPI100 Δ*bamA::cat* pZS21-*bamA*$^{+}$, Cm^{R} Kan^{R}	(Ruhe et al., 2013b)
CH10024	EC93 *cdiA(A2909)*	This study
CH10053	EC93 *bamA*^{LT2}*::kan*, Kan^{R}	(Ruhe et al., 2014)
CH10060	EC93 *bamA*^{LT2}	This study
CH10094	EC93 Δ*cdiA*	(Ruhe et al., 2014)
CH10131	EC93 *bamA*^{LT2} Δ*cdiI::kan*, Kan^{R}	This study
CH10151	EC93 *bamA*^{LT2} Δ*cdiI*	This study

[a]Abbreviations: Amp^{R}, ampicillin-resistant; Cm^{R}, chloramphenicol-resistant; Kan^{R}, kanamycin-resistance; Rif^{R}, rifampicin-resistant; Tet^{R}, tetracycline-resistant

Table 3

Plasmids

Plasmid	***Description*** [a]	***Reference***
pTrc99a	IPTG-inducible expression plasmid, Amp^R	GE Healthcare
pCH450	pACYC184 derivative with *E. coli araBAD* promoter for arabinose-inducible expression, Tet^R	(Hayes & Sauer, 2003)
pSIM6	Expresses phage λ Red proteins from heat-shock inducible promoter, Amp^R	(Datta *et al.*, 2006)
pKAN	pBluescript with FRT-flanked kanamycin-resistance cassette ligated into SmaI restriction site, Amp^R Kan^R	(Hayes & Sauer, 2003)
pKAN-BamA(KO)	pKAN containing regions upstream and downstream of $bamA^{Eco}$, Amp^R Kan^R	This study
pWEB-TNC	Cosmid cloning vector, Amp^R Cm^R	Epicentre
pDsRedExpress2	Constitutive expression of DsRed, Amp^R	Clontech
pDAL741	pBR322 derivative that expresses $cdiI^{EC93}$ immunity gene, Amp^R	(Aoki et al., 2005)
pCP20	Heat-inducible expression of FLP recombinase, Cm^R Amp^R	(Cherepanov & Wackernagel, 1995)
pSH21P	pET21b-derived expression plasmid, appends an N-terminal His_6 epitope tag, Amp^R	(Koskiniemi *et al.*, 2014)
pCH450-DsRed	L-arabinose inducible expression of DsRed, Tet^R	This study
pTrc99A-sfGFP	IPTG inducible expression of superfolding GFP, Amp^R	This study
pCH450-GFP	L-arabinose inducible expression of superfolding GFP, Tet^R	This study
pKAN-*cdiAΔCT*	Construct to delete the *cdiA-CT* region from *E. coli* EC93, Amp^R Kan^R	This study
pKAN-Δ*cdiI*	Construct to delete the *cdiI* immunity gene from *E. coli* EC93, Amp^R Kan^R	This study
pZS21	pSC101-derived plasmid vector, Kan^R	(Lutz & Bujard, 1997)
pZS21-$bamA^+$	pZS21 derivative that expresses $bamA^{Eco}$, Kan^R	(Kim *et al.*, 2007)
pZS21-$bamA^{ECL}$	Expresses $bamA^{ECL}$ from *Enterobacter cloacae* ATCC 13047, Kan^R	(Ruhe et al., 2013b)
PDAL660Δ1-39	Constitutive expression of the $cdiBAI^{EC93}$ gene cluster, Cm^R Amp^R	(Aoki et al., 2005)
pDAL878	Derivative of pDAL660Δ1-39 in which the *cdiA-CT/cdiI* region has been deleted. Produces truncated CdiA(V2905stop) protein, Cm^R Amp^R	(Webb et al., 2013)
pCH12699	Derivative of pDAL660Δ1-39 that produces CdiA(ΔG722-G1624), Cm^R Amp^R	This study
pCH12700	Derivative of pDAL660Δ1-39 that produces CdiA(ΔG722-Y1697), Cm^R Amp^R	This study
pCH12702	Derivative of pDAL660Δ1-39 that produces CdiA(ΔG277-G721), Cm^R Amp^R	This study
pCH12703	Derivative of pDAL660Δ1-39 that produces CdiA(ΔS633-G721), Cm^R Amp^R	This study
pCH12704	Derivative of pDAL660Δ1-39 that produces CdiA(ΔS644-G721), Cm^R Amp^R	This study
pCH12705	Derivative of pDAL660Δ1-39 that produces truncated CdiA(R2123stop), Cm^R Amp^R	(Aoki et al., 2005)
pCH12706	Derivative of pDAL660Δ1-39 that produces truncated CdiA(R1930stop), Cm^R Amp^R	(Aoki et al., 2005)
pCH12707	Derivative of pDAL660Δ1-39 that produces truncated CdiA(R1319stop), Cm^R Amp^R	(Aoki et al., 2005)
pCH12732	IPTG-inducible expression of $cdiBAI^{EC93}$ gene cluster, Cm^R Amp^R	This study
pCH12736	Derivative of pDAL660Δ1-39 that produces truncated CdiA(N2556stop), Cm^R Amp^R	(Aoki et al., 2005)

[a] Abbreviations: Amp^R, ampicillin-resistant; Cm^R, chloramphenicol-resistant; Kan^R, kanamycin-resistance; Rif^R, rifampicin-resistant; Tet^R, tetracycline-resistant